

The behaviour of anchor plates in clay

R. K. ROWE* and E. H. DAVIS†

The undrained behaviour of anchor plates with a vertical or horizontal axis, resting in a saturated clay, is examined. Theoretical consideration is given to the effects of anchor embedment, layer depth, overburden pressure and breakaway condition as well as anchor roughness, thickness and shape. The influence of these parameters on the failure mechanism and the anchor capacity is discussed. It is shown that in many cases ultimate collapse is preceded by significant anchor displacement and a definition of failure which allows reasonable displacement predictions to be made at working loads is proposed. Model tests for anchors with a vertical axis are reported. A comparison of these results and other published data with the theoretical solutions indicates encouraging agreement. The results of this study are presented in the form of charts which may be used directly in hand calculations for estimating the undrained failure load for anchor plates.

L'article décrit le comportement non-drainé des plaques d'ancrage à axe vertical ou horizontal qui reposent dans l'argile saturée et décrit du point de vue théorique les effets de l'encastrement de l'ancrage, de la profondeur des couches, de la pression du terrain de couverture de la rugosité de l'épaisseur et de la forme de l'ancrage. L'influence exercée par ces paramètres sur le mécanisme de rupture et la charge utile de l'ancrage sont aussi discutées. On démontre que dans beaucoup de cas la rupture finale est précédée d'un déplacement significatif de l'ancrage et on propose une définition de la rupture qui facilitera la prévision raisonnable des déplacements sous charges de service. Un compte-rendu est donné de tests-modèles pour les ancrages à axe vertical. Une comparaison de ces résultats et d'autres données déjà publiées avec les solutions théoriques indique une correspondance encourageante. Les résultats de cette étude sont présentés sous la forme d'abaques qui peuvent être employés de façon directe dans des calculs manuels pour évaluer la charge de rupture des plaques d'ancrage dans des conditions.

INTRODUCTION

The solution of many civil engineering problems requires a prediction of the behaviour of buried structures. Frequently these buried structures may be idealized as an anchor plate. Such structures include anchors or buried footings used to support transmission towers, retaining walls, bridges and

tension roofs, as well as submerged pipelines subject to uplift pressures.

The prediction of anchor plate behaviour is usually restricted to the limiting conditions of elastic displacement (e.g. Fox, 1948; Douglas & Davis, 1964; Rowe & Booker, 1979a, 1979b) or ultimate capacity (e.g. Meyerhof & Adams, 1968; Vesic, 1971). Elastic solutions may be conveniently used for estimating displacements provided that the load-deflexion response within the working load range is quasi-linear. However, this condition will be satisfied only if there is limited local yield within the material. In general, the extent of local yield will depend on material properties, the initial stress state, the boundary conditions at the anchor interface and the load level relative to the collapse load.

Many investigators have proposed approximate techniques for determining the collapse load for anchor plates. Most approaches involve the use of either limit equilibrium concepts or the method of characteristics, frequently combined with empirical corrections (e.g. Meyerhof & Adams, 1968; Balla, 1961; Vesic, 1971). Others (e.g. Ladanyi & Johnston, 1974; Vesic, 1971) have proposed different uses of cavity expansion theories for predicting anchor capacity. None of these approaches provides a rigorous solution to the general problem of predicting the ultimate capacity of anchor plates (although a number of the approaches have been successfully used for specific cases).

The finite element method provides a convenient means of analysing the load-deflexion behaviour of anchor plates up to collapse, and allows consideration of many factors excluded from other analyses. Several authors (e.g. Ashbee, 1969; Davie & Sutherland, 1977) have performed finite element analyses for circular anchor plates but no general study appears to have been attempted.

In this Paper a finite element study of the undrained behaviour of anchor plates in homogeneous, isotropic saturated clay is reported; the results are compared with the Authors' model tests and other available experimental data. In a companion paper (Rowe & Davis, 1982) consideration is given to anchor plates in sand as well as anchors in a cohesive-frictional soil. In both papers emphasis is placed on the effect of local yield on the load-deflexion response and in some cases the adoption

Discussion on this Paper closes 1 June 1982. For further details see inside back cover.

* University of Western Ontario.

† Formerly University of Sydney, now deceased.

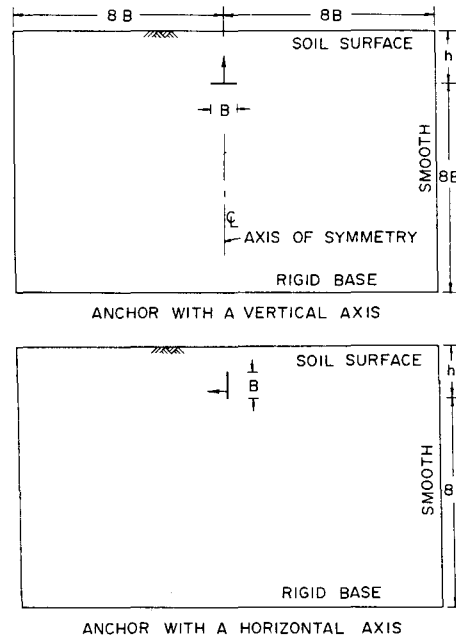


Fig. 1. Problem analysed

of a displacement-related practical failure load (which may be less than or equal to the collapse load) is advocated.

Attention is largely directed towards predicting the behaviour of strip anchor plates of width B , buried to a depth h , with both vertical and horizontal loading as indicated in Fig. 1. Consideration is then given to the effect of anchor thickness and shape. The results are presented in the form of charts which may be used in hand calculations for determining design failure loads.

NUMERICAL ANALYSIS

The numerical solutions presented in this Paper were obtained from an elasto-plastic finite element analysis using the soil-structure interaction theory described by Rowe, Booker & Balaam (1978). This substructure approach allows consideration of plastic failure within the soil, anchor breakaway from the soil behind the anchor, and shear failure at a frictional dilatant soil-structure interface without the introduction of special joint or interface elements.

For the purposes of this study, the anchor was assumed to be thin and perfectly rigid. The main analysis was for plane strain conditions, so that the anchor is considered to be an infinite strip. A limited number of analyses were performed for axisymmetric conditions. The soil was assumed to have a Mohr-Coulomb failure criterion.

The finite element boundary conditions are shown in Fig. 1. The case of an anchor at infinite

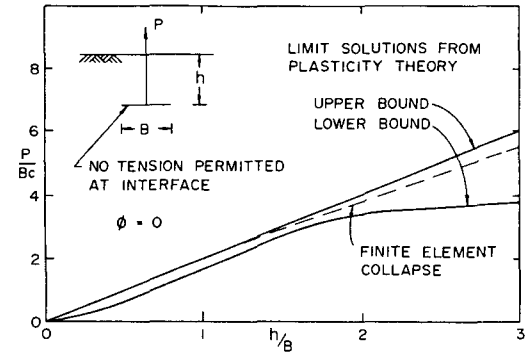


Fig. 2. Limit solutions for a shallow anchor; no interface tension

depth was analysed by specifying rigid boundaries at a distance of eight anchor widths in each direction. The finite element mesh consisted of 670-1200 constant strain elements (depending on geometry) arranged in a crossed triangular configuration as advocated by Nagtegaal, Parks & Rice (1974).

To ensure that the behaviour of the singularity at the anchor tip was modelled as accurately as possible, a technique of introducing potential rupture lines (Rowe & Davis, 1977) near the edge of the anchor was adopted. This approach attempts to overcome the inhibition of free plastic flow inherent in the usual stiffness formulation of the finite element method by permitting the formation of velocity discontinuities in the regions of high stress and velocity gradient near the tip of the anchor plate. A description and justification of this technique, and numerical checks on incremental procedure, load step size and convergence are given by Rowe (1978).

The finite element results obtained from this study were compared with available benchmark solutions from elasticity (e.g. Douglas & Davis, 1964; Rowe & Booker, 1979a, 1979b) and plasticity theory and were found to be in reasonable agreement. For example, in Fig. 2 the finite element collapse load is compared with the best available upper and lower bounds for an anchor in a weightless, purely cohesive soil for the condition of no tension at the anchor interface. Although the exact collapse load is not known for this problem, there is good agreement with the limit solutions in regions of close bounding.

The finite element collapse loads obtained for the limiting cases of a surface footing and a smooth vertical retaining wall in a purely cohesive material were 4.3% and 2.5% above the analytical collapse loads of $5.14Bc$ and $2Bc$ respectively. The numerical collapse load for a fully bonded anchor at infinite depth exceeded the best available upper bound of $11.42Bc$ by 4.6%. The load-deflexion

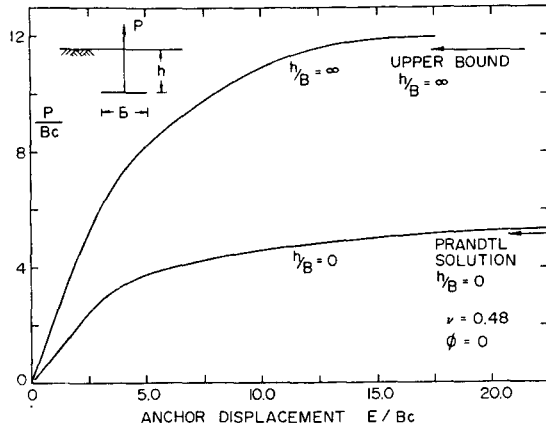


Fig. 3. Load-displacement curves for two rigid anchors; fully bonded

curves for the limiting cases of a fully bonded anchor with a vertical axis are shown in Fig. 3. The close agreement between the numerical and analytical loads for these cases suggests that the numerical collapse loads for intermediate embedment ratios could be expected to be within 5% of the actual collapse load. In fact, if the numerical collapse loads for the fully bonded anchor are all reduced by 5% then the finite element results lie between the best available upper and lower bound solutions (Rowe, 1978), as shown in Fig. 4.

THEORETICAL RESULTS

Anchor capacity

The average applied pressure q_u required to cause undrained failure of an anchor plate in a saturated clay with cohesion c and $\phi_u = 0$ may be expressed in the form

$$q_u = cF_c' \quad (1)$$

where F_c' is the lower value given by

$$F_c' = F_c + sq_h/c \quad (2a)$$

or

$$F_c' = F_c^* \quad (2b)$$

where F_c is the dimensionless anchor capacity factor corresponding to the case where the soil is initially stress-free and the interface between the back of the anchor and the soil is incapable of sustaining tension, i.e. is unbonded. Under these conditions there will be immediate breakaway of the soil from the back of the anchor as soon as load is applied. F_c^* is the dimensionless anchor capacity factor for an anchor which is fully bonded to the surrounding soil. By definition, there can be no breakaway between the anchor and the soil. This situation would arise if the interface could sustain tension due to suction or adhesion or if the initial stresses were sufficiently large to ensure that the

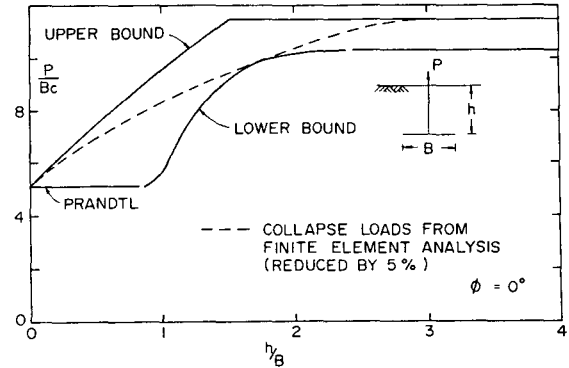


Fig. 4. Limit solutions for a fully bonded anchor with a vertical axis

stresses behind the anchor were compressive for all anchor loads up to and including the failure load. q_h is the overburden pressure at depth h and s is a coefficient for the effect of overburden pressure on anchor capacity.

For intermediate levels of initial stress, breakaway will occur when the compressive stress behind the anchor is reduced to zero. Under these conditions, the value of F_c' will be between the limiting values of F_c and F_c^* and will depend on the initial overburden pressure q_h and, for anchors with a horizontal axis, the initial stresses acting normal to the anchor plate $K_0 q_h$. The transition between F_c and F_c^* can be given in terms of s in equation (2a).

Definition of failure: the k_4 failure concept

Finite element analyses were performed to obtain the anchor capacity factors for a range of embedment ratios. These analyses indicated that although clearly defined collapse loads could be obtained, in many cases the deformation due to contained plastic flow before collapse was so great that, for practical purposes, failure would be deemed to have occurred at a load well below the collapse load.

The effect of local yield (contained plasticity) on surface footing behaviour has long been recognized. Terzaghi (1943), for example, defined local shear failure in terms of the load at which the load-deflection curve passes into a steep straight tangent; Terzaghi & Peck (1967) recommend values of c and $\tan \phi$ reduced to two thirds of their measured values in bearing capacity theory when dealing with loose or soft soils which exhibit this type of behaviour. D'Appolonia, Poulos & Ladd (1971) have used the finite element to show the importance of local yield on the displacement of foundations in soft clay.

The results of model and field tests on anchor plates suggest the presence of significant contained plastic deformation before collapse and failure is

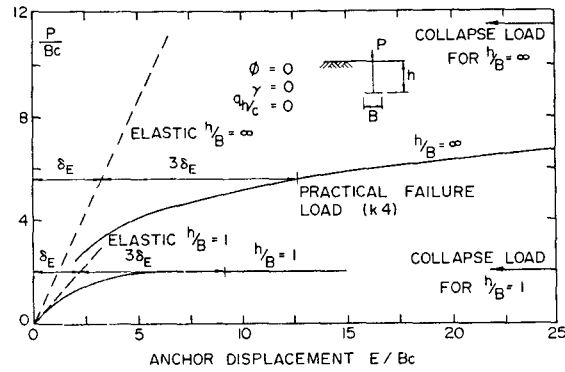


Fig. 5. Definition of failure

often defined according to an arbitrary rule, such as load at a specified displacement, or according to Terzaghi's (1943) local yield criterion. A loading path finite element analysis provides a convenient means of identifying this effect more clearly. For example, load-deflexion curves obtained for two anchors with a vertical axis are shown in Fig. 5 for the immediate breakaway condition. The collapse load for a deep anchor ($\phi = 0$) is independent of the initial stress conditions; however, the deformation before collapse varies considerably. In the case of immediate breakaway, there is significant local yield at low load levels ($P/Bc > 3$) and the load-deflexion curve passes into a steep, relatively straight tangent as the plastic region gradually expands until collapse is reached after a very large displacement. For such cases, the use of the true collapse load in conjunction with typical factors of safety of 2.5–3 would give working loads in the non-linear range of behaviour and would result in displacements much larger than would be predicted from elastic analyses and probably larger than practically acceptable.

This suggests the need for a practical definition of failure for problems in which the full ultimate capacity is obtained only after extensive contained plastic deformation. Although many such definitions have been used, a definition that is convenient and rational in the present context is that the failure load is considered to have been reached when the displacement is a selected multiple of that which would have been reached had conditions remained entirely elastic. This definition is arbitrary in terms of the choice of multiple to be used; however, it is not dependent on scale or modulus and it gives a calculable limit on the displacement before failure, provided the load path to failure is monotonic. In this Paper, 4 is chosen as the multiple and the failure load is denoted as the k_4 failure load; it corresponds to an apparent stiffness of one quarter of the elastic stiffness. (Similarly k_2 and k_3 are loads correspond-

ing to an apparent stiffness of one half and one third respectively of the elastic stiffness.) The adoption of a multiple of 4 in conjunction with a typical factor of safety of 2.5–3 will generally ensure that the working load is close to the linear range and hence the displacement may be estimated from elastic solutions. Creep effects increase with increasing contained plasticity within the soil and hence the adoption of the k_4 practical failure load will minimize the contained plasticity and creep at working loads.

Not all anchors exhibit large deformations before collapse. In particular, for shallow anchors with a vertical axis and for fully bonded anchors, the k_4 practical failure load is identical with the ultimate collapse load. This can be seen for $h/B = 1$ in Fig. 5.

Limiting cases: immediate and no breakaway conditions—smooth anchor

Dimensionless anchor capacity factors F_c and F_c^* determined for the limiting cases of immediate breakaway and no breakaway are shown in Figs 6 and 7 for anchor plates with vertical and horizontal axes respectively. The anchor capacity factors determined from the actual collapse load are indicated by a full line; those determined using a practical (k_4) definition of failure are denoted by long dashed lines. In these cases where contained plastic deformation governs the anchor response, the dimensionless loads corresponding to two, three and five times the elastic displacement are shown by short dashed lines, to indicate the sensitivity of the anchor capacity factor to the definition of the practical failure load.

Anchors may be classified as shallow or deep, depending on the nature of the anchor response. A deep anchor is not appreciably affected by the proximity of the soil surface and any increase in embedment beyond the critical embedment at which the anchor is first classified as being deep will not have a significant effect on the anchor capacity. Anchors with a vertical axis exhibit deep anchor behaviour for embedment ratios greater than about 4 for the immediate breakaway cases and about 3 for the no breakaway case. Anchors with a horizontal axis have a critical embedment ratio of 3 for both breakaway conditions.

The effect of embedment depth and breakaway condition on anchor behaviour is evident from the plastic region and velocity fields at failure shown in Figs 8–12. In these figures, failure corresponds to the k_4 failure load, where applicable, as indicated by the dashed lines in Figs 6 and 7.

Figure 8 indicates that for the immediate breakaway case, failure of a shallow anchor with a vertical axis is associated with the development of a limited shear zone near the edge of the anchor

and an almost rigid upward movement of a block of soil directly above the anchor. Here, the failure involves complete collapse. Under similar conditions, failure of a very deep anchor is due to extensive contained plastic deformation and significant additional plastic failure would be required to achieve complete collapse. Fig. 9 shows the failure mechanisms for the corresponding no breakaway case. Here k_4 failure coincides with ultimate collapse for both shallow and deep anchors. Plastic flow extends to the soil surface for the shallow anchor and from front to back for the very deep anchor.

The failure mechanism for an intermediate case ($h/B = 3$), corresponding to the transition from shallow to deep anchor behaviour, is shown in Fig. 10. Although the behaviour of this anchor is influenced by the presence of the free surface, the failure load is very close to that of an infinitely deep anchor. In particular, the velocity field for the no breakaway case shows that collapse is predominantly associated with plastic flow from the front to the back of the anchor.

The behaviour of an anchor with a horizontal axis is in many respects similar (and for a very deep anchor is identical) to that of anchors with a vertical axis. The transition from shallow to deep anchor behaviour occurs at an embedment ratio of about 3 as indicated by Figs 11 and 12. Shallow anchor ($h/B = 1$) failure is characterized by plastic flow to the soil surface. For a deeper anchor ($h/B = 3$) failure is more contained, and in the no breakaway case involves plastic flow from front to back.

Intermediate breakaway cases: smooth anchors

For an anchor where the interface between the back of the anchor and the soil is incapable of sustaining tension (i.e. unbonded), the immediate breakaway and no breakaway conditions already discussed correspond to the limiting cases where the initial overburden pressure q_h is zero and very large respectively. Finite element analyses indicate that the overburden pressure required to ensure a no breakaway response for a homogeneous elastoplastic material is approximately $6c$ for anchors

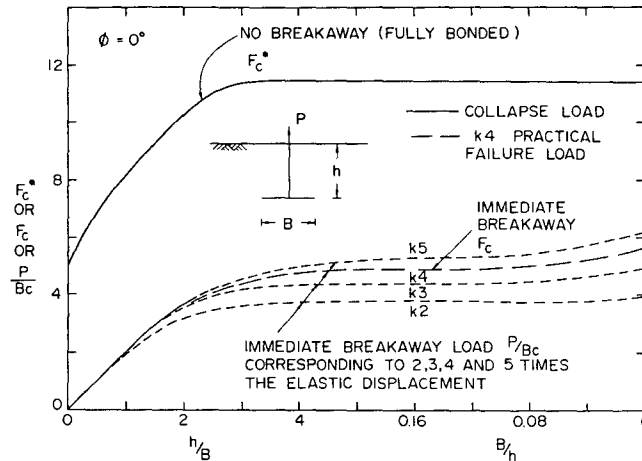


Fig. 6 (top left). Variation of anchor capacity factors with embedment ratio

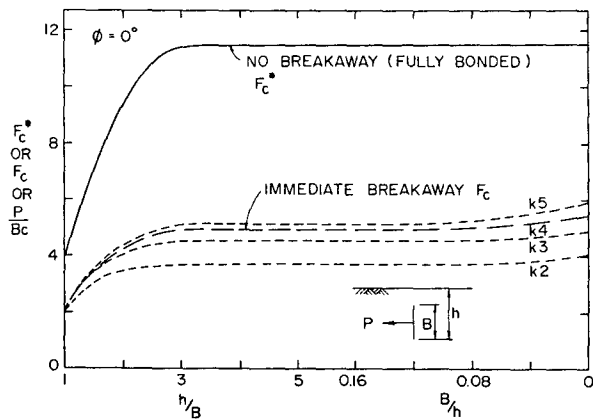


Fig. 7 (bottom left). Variation of anchor capacity factors with embedment ratio

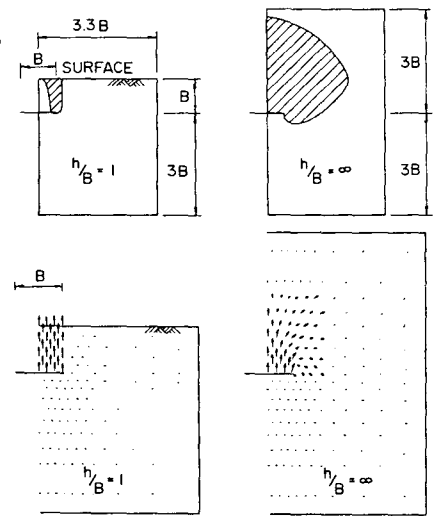


Fig. 8 (below). Plastic regions and velocity fields at collapse; immediate breakaway

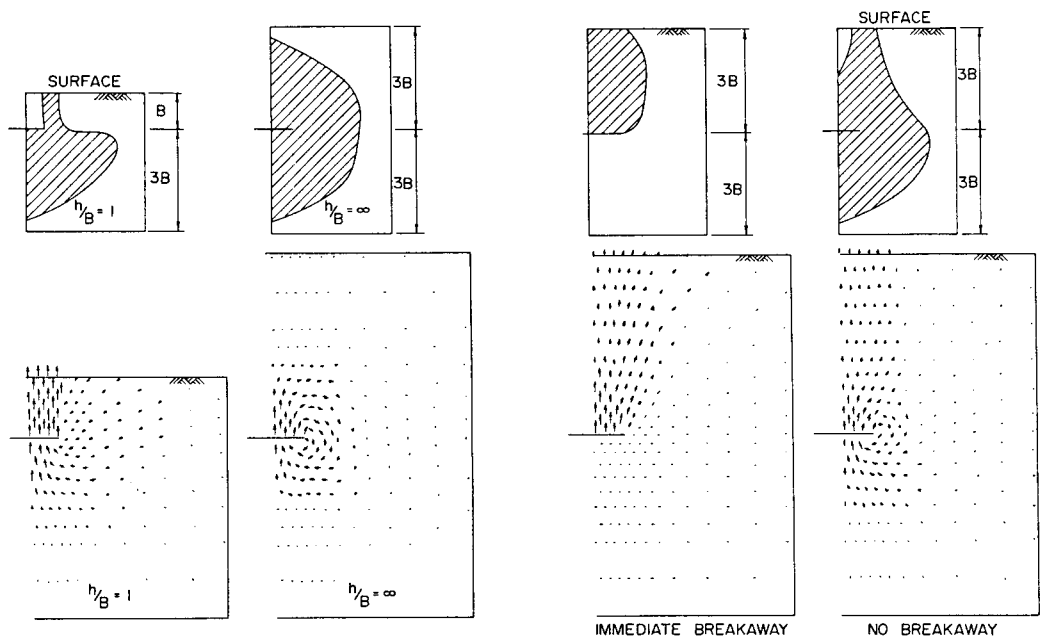


Fig. 9 (below left). Plastic regions and velocity fields at failure; no breakaway (fully bonded)

Fig. 10 (below right). Effect of breakaway on plastic regions and velocity fields at failure; $h/B = 3$

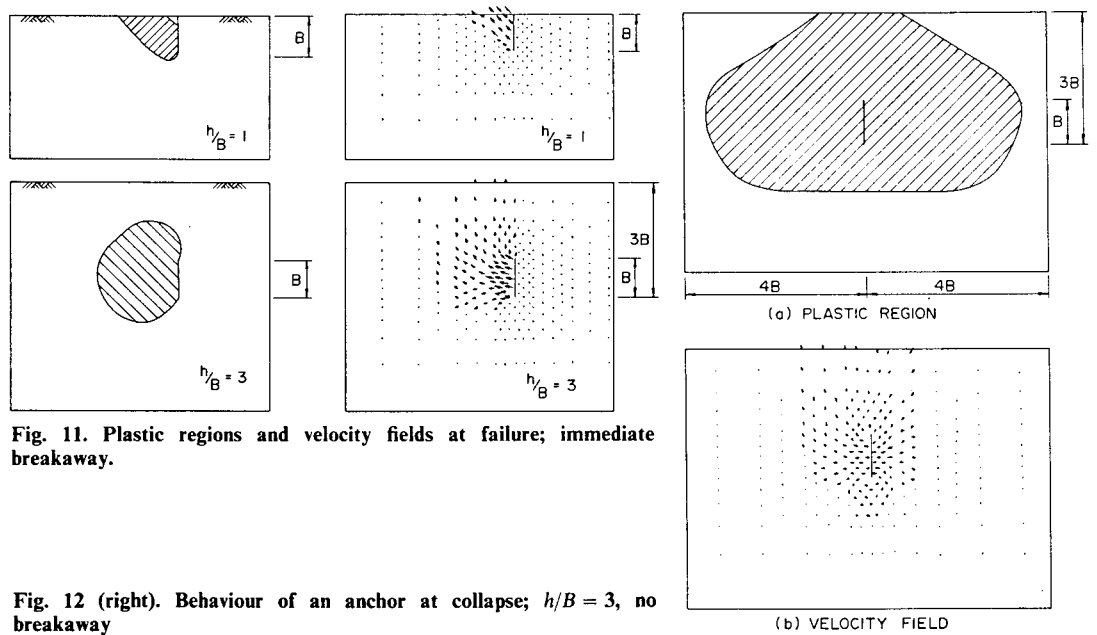


Fig. 11. Plastic regions and velocity fields at failure; immediate breakaway.

Fig. 12 (right). Behaviour of an anchor at collapse; $h/B = 3$, no breakaway

with a vertical axis and typically ranges between $4c/K_0$ and $6c/K_0$ for anchors with a horizontal axis. Results (Ladd & Edgers, 1972) for a number of clays suggest that the dimensionless overburden pressure q_h/c will often lie in the range $6 \leq q_h/c \leq 12$ for normally consolidated clays down to $1 \leq q_h/c \leq 2.5$ for highly overconsolidated clays ($OCR = 10$). Thus, situations will commonly arise in which the initial overburden pressure lies between the limiting values required to achieve either an immediate or no breakaway response. For these intermediate cases, the anchor response will initially be as if it were fully bonded. However, breakaway from the soil behind the anchor will occur some time during the loading sequence.

The increase in anchor capacity with overburden pressure is shown in Fig. 13. Anchor capacity may be considered to increase linearly with overburden pressure between the limits imposed by the immediate and no breakaway cases. Thus, the anchor capacity factor can be given by equation (2a), where the factor s corresponds to the rate of increase in anchor capacity with overburden pressure. For anchor systems with a vertical axis, s may be taken to be unity and at least approximately independent of K_0 .

For anchors with a horizontal axis and hydrostatic initial stress conditions ($K_0 = 1$), s varies with embedment ratio from $s = 0.5$ for $h/B = 1$ to $s = 0.96$ for $h/B = 3$. The value of s for intermediate embedments may be obtained by linear interpolation. For deep anchors ($h/B > 3$) s may be taken to be unity. For anchors with a horizontal axis and non-hydrostatic initial stress conditions, the value of s is approximately equal to K_0 times the value obtained for hydrostatic conditions.

Full ultimate collapse load for deep anchors in a purely cohesive soil is independent of the initial stress state within the soil mass, and hence is independent of the breakaway condition. However, the extent of plastic deformation before collapse is highly dependent on the initial overburden stress, and the practical failure load increases in direct relation to the overburden pressure up to the limiting no breakaway condition as shown in Fig. 13. Although this variation is not entirely linear, to sufficient accuracy, it may be approximated by a straight line with a slope s equal to unity as previously indicated. (The slight difference between the results for deep anchors with horizontal and vertical axes arises from the difference in the refinement of the finite element meshes used in the different analyses.)

The load-deflexion curves obtained for the intermediate breakaway cases are identical to the no breakaway curves, until breakaway occurs. Full breakaway is accompanied by extensive plastic deformation and the practical failure load is gener-

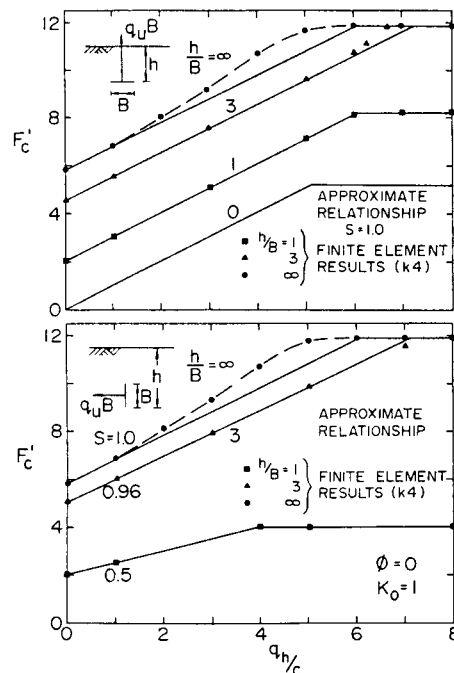


Fig. 13. Variation in anchor capacity with overburden pressure q_h/c

ally obtained shortly after full breakaway. Thus, working loads deduced by applying a factor of safety of 2.5–3 to the anchor capacity given by equations (1) and (2) typically correspond to the no breakaway portion of the load-deflexion response. Thus, for a homogeneous soil and an overburden pressure q_h/c greater than unity, it would generally be appropriate to estimate the working load deflexions from elastic solutions for a fully bonded anchor.

Adhesion and/or suction

Suction or adhesion between the back of the anchor and the soil will give rise to a no breakaway response until cavitation occurs or the adhesive strength of the interface bond is exceeded. Once breakaway occurs, the stress redistribution arising from the loss of adhesion or suction will lead to an appreciable increase in displacement. The failure load for this case may be estimated from equation (1) where $F'_c = F_c + q_a/c$ and q_a is the available adhesion or suction. However, because of the effect of stress redistribution after breakaway and the uncertainty as to the actual magnitude of adhesion and suction that may be mobilized, it is suggested that particular caution should be adopted in any anchor design which relies on suction or adhesion. Estimation of the magnitude of q_a can be much more important in interpreting tests on a model scale than for field scale design.

